Dynamics of a Point Absorber Wave Energy Converter

Curtis J. Rusch, Daniel R. Green, Derek S. Sager, Jared D. McGarry, Jonathan T. Morasch, Joseph A. Downs

UW WEC Team, Department of Mechanical Engineering, University of Washington, Seattle, WA 98195-2600, USA

A B S T R A C T

A small scale, modular, wave energy converter (WEC) was constructed for use as a testing platform for various WEC designs and component configurations. The WEC is optimized for operation in scale conditions (H = 0.5 m, T = 3 s). The WEC was tested on a lake to characterize its reaction to a vessel wake as a proxy for a wave field. A qualitative analysis of the WEC response to these waves is presented, which set the stage for future testing in a natural wave field.

1 Introduction

As energy demands increase and concerns over the environmental impact of current energy production grow, renewable energy sources are looked upon as a viable and necessary alternative. The wave energy resource has been the focus of recent studies, including one that estimates there is 2,640 TWh/yr of theoretically available wave energy along the outer continental shelf of the United States. The technically available resource is lower, around 1,170 TWh/yr, but is substantial compared to electrical power generation of 4,000 TWh/y in the U.S. [1]. This makes wave energy converters (WECs) an important aspect of future power production. The WEC presented in this paper is of the "point absorber" classification. A point absorber is a wave energy device with dimensions small in comparison to the incident wavelength, but the point absorber is able to convert energy from a wave front larger than the characteristic dimension of itself [2].

The University of Washington Wave Energy Converter team was tasked with designing and building a small-scale point absorber WEC for research purposes. A driving requirement is that the WEC should be modular, to allow for easy modifications and development of future designs. This paper characterizes the resulting point absorber WEC.

2 System Overview

This point absorber WEC consists of three major components: a buoy, a heave plate connected to the buoy by a flexible line, and a power take-off system inside the buoy. The WEC generates power when wave excitation of the buoy produces opposing motion and forces between the buoy and heave plate, which are harnessed by the power take-off system.

2.1 Buoy

The buoy consists of a buoyant shell (0.057 m^3, 15 gallon drum), housing a hydraulic cylinder, a spring, and an Amsteel line connecting the piston to the heave plate. These are oriented in series along the vertical centerline, as shown in Fig. 1. The remaining volume within the buoy is filled with urethane foam to prevent sinking in case of water ingress. A urethane foam-filled ring is fastened around the outside of the buoy shell for added buoyancy. To increase passive stability, a 15.88 kg (35 lb) cast iron mass is attached to the bottom of the buoy, positioning the center of mass below the center of buoyancy.

2.2 Power Take-Off

The WEC buoy houses a double-acting hydraulic system that uses a spring to keep the line in tension. The hydraulic system uses four low-pressure check valves to alternate between supply and output at either end of the hydraulic cylinder. A pressure gauge is mounted on the output side before a flow restrictor (adjustable needle valve) in order to control the pressure as a function of

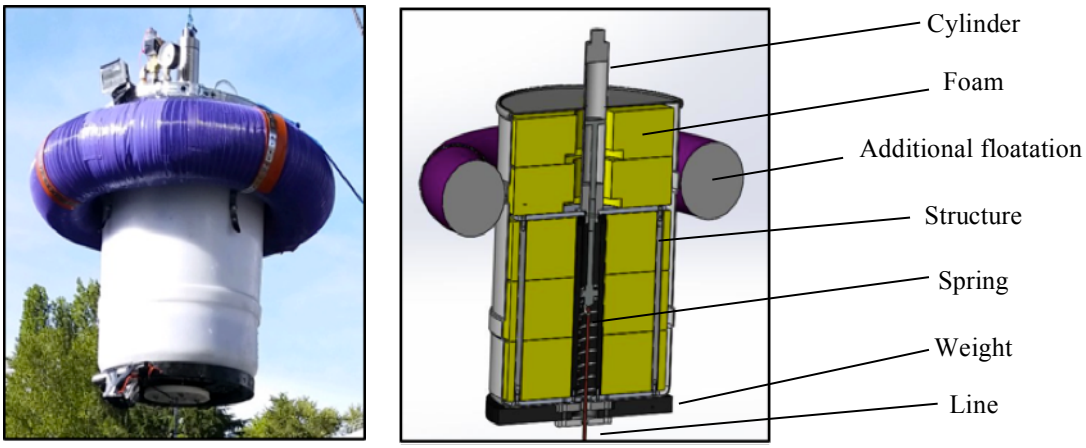

Fig. 1. (Left) Photo of complete buoy, and (right) a cut-through view of a model showing the buoy interior.

flow, as shown in Fig. 2. Fresh water is used as the hydraulic fluid due to its low viscosity and negligible environmental impact, in the event of a leak. The piston is a 51 mm (2 inch) bore cylinder with 230 mm (9 inch) stroke. 13 mm (0.5 inch) tubing is used.

2.3 Heave Plate

The purpose of the heave plate is to provide a counter force to the buoy, through the means of weight and drag. The heave plate consists of a steel rod fastened to a steel plate. Cast iron weights slide over the steel rod, allowing easy modification of the overall heave plate mass. A parabolic bowl with a center hole slides over the center rod and is clamped atop the barbell weights, as shown in Fig. 3.

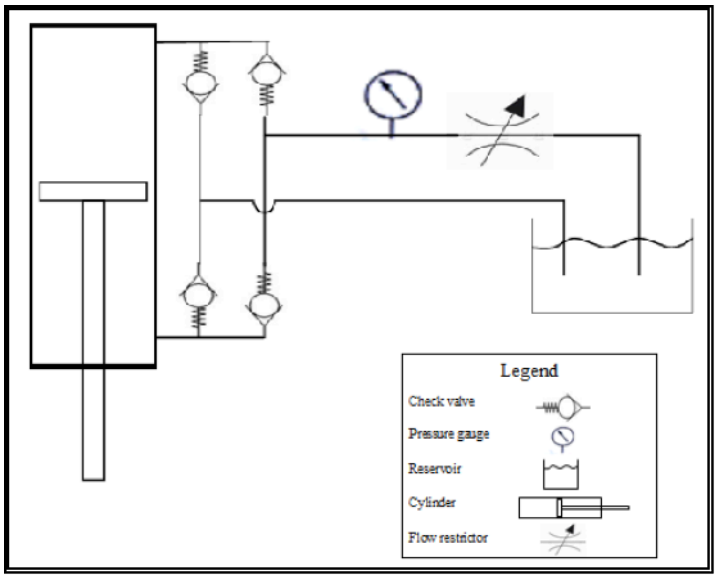

Fig. 2. Schematic of hydraulics system

Fig. 3. Picture of assembled heave plate

3 Methods

3.1 Instrumentation

The instrumentation used for the dock testing and the lake testing consisted of pressure loggers (Onset) and inertial measurement units (x-IO Technology's x-IMU) to monitor the motion of the buoy and the heave plate, and cameras (GoPro) to give visual feedback while the device was deployed. The pressure loggers captured data at 1 Hz, the IMUs at 256 Hz, and the cameras at 30 Hz (30 frames per second). Instruments operated autonomously and time synchronization was conducted *post hoc*.

The pressure loggers recorded a time sequence of the pressure, which was then converted to depth as

$$h = \frac{P}{\rho g} \qquad (1)$$

where P is the pressure (Pa), ρ is the density of the water (1000 kg/m^3), g is the acceleration due to gravity (9.81 m/s^2), and h is the depth (meters).

The IMUs recorded acceleration as a function of time in the X, Y, and Z directions, in the IMU frame of reference. To extract information on the positions of the heave plate and buoy from the raw IMU data, a variety of open-source MATLAB code was used [3]. This code uses an attitude and heading reference system (AHRS) algorithm, which determines the orientation of the IMU's reference frame relative to the Earth's reference frame [4]. Position is calculated by double integration of acceleration data in the earth coordinate frame with intermediate high pass filtering to reduce the effect of noise.

The pressure loggers were secured to the WEC, one to the bottom of the buoy and one just above the top of the heave plate (see appendix, Fig. A.1 and Fig. A.2). The IMUs were placed in spare GoPro cases. One was secured just above the top of the heave plate, and one secured on top of the buoy. One GoPro camera was secured to the top of the buoy, and positioned to watch the hydraulic pressure gauge (see appendix, Fig. A.3). Another camera was secured to the bottom of the buoy and oriented to monitor for slack in the line connecting the buoy and heave plate.

3.2 Field Testing

The system was deployed in the northern part of Lake Washington. A motorboat was used to create wakes around the WEC, in the absence of natural waves of significant height. Attempts were made to measure the incoming waves using SWIFTs (Surface Wave Instrument Floats with Tracking), but without a long-lived, regular wave field, information from these devices proved to be uninformative. Wakes usually hit the buoy in groups of three waves, a pattern that will be shown in the results section.

3.3 Hydraulic Power Output

To calculate the efficiency of the system, the power generated by the buoy must be determined (Power = Pressure x Flow Rate). By stepping through the GoPro video, of which a still shot can be seen in Fig. 4, hydraulic pressure data can be obtained at 30 Hz. Using the data obtained from the flow determination experiment described in Section 4.1, a line of fit was used to relate the pressure seen on the gauge to the flow

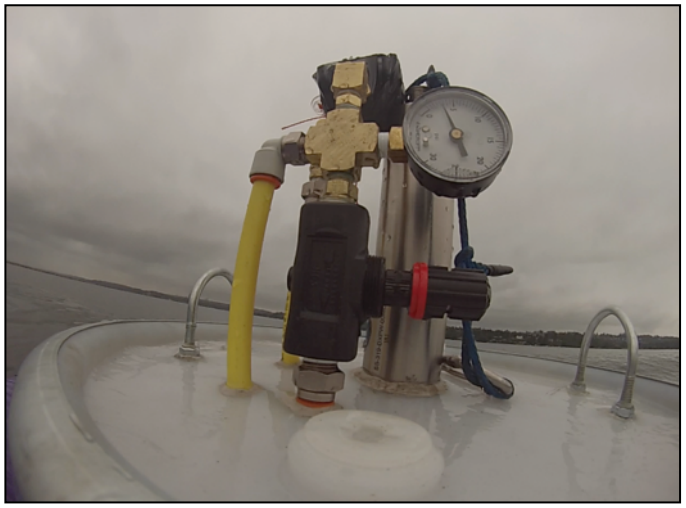

Fig. 4. Still shot from GoPro footage taken during testing

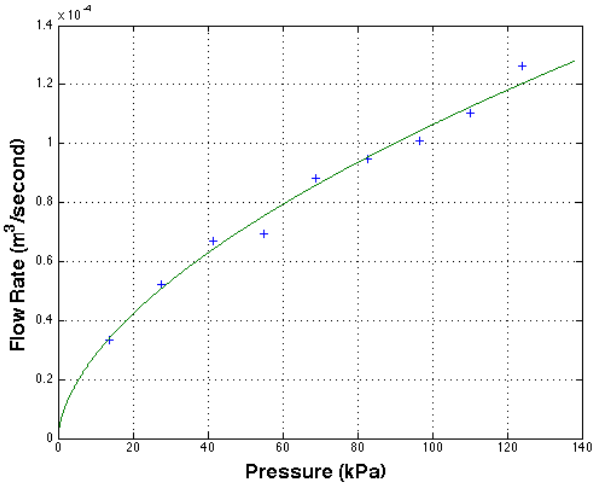

Fig. 5. Flow rate as a function of pressure for black/grey setting from bench testing, overlaid with a line of fit.

rate in the system. This plot can be seen in Fig. 5 (above), and shows the relation between pressure and flow rate for the needle valve setting used in testing. From this data, the instantaneous power can be calculated at 30 Hz for the duration of the test.

3.4 Capture Width Definition

Capture width is one measure by which the performance of a heaving point absorber can be characterized. Capture width is the width of a wave crest that contains the same power as is extracted from the waves by a WEC, and is calculated as

$$l = \frac{P}{P_{wave}} \qquad (2)$$

where l is the capture width (meters), P is the power absorbed by the WEC (W), and P_{wave} is the incident wave power (W/m of crest). Here, the power output

from the PTO is used to evaluate capture width, in place of the absorbed power.

3.5 Heave Plate Dynamics

The drag force created by the heave plate F_d is determined as

$$F_d = c_d \left(\frac{1}{2}\right) \rho v^2 A \qquad (3)$$

where c_d is the drag coefficient determined by the shape of the body, ρ is the density of water (kg/m^3), v is the velocity of the flow (m/s), and A is the frontal area of the body (m^2). As the heave plate is asymmetric, c_d varies depending on the direction of heave plate motion. These values are shown in Section 4.6.

4 Results

4.1 Flow Determination

The performance of the WEC is evaluated through the analysis of the power output. In order to obtain power data, the flow rate in the system must be known. As there is no flow meter on board the system, testing of the needle valve was conducted to determine the relationship between pressure and flow rate at discrete settings as shown in Table 1.

The bench testing consisted of flowing fresh water through the needle valve and monitoring the flow rate and pressure as shown in Fig. 6. Using the black/grey setting (which generates the highest power), a line of fit was generated to approximate the data. The plot of experimental data and the line of fit can be seen Fig. 5.

Table 1. Needle valve setting optimization

Band	Pressure (kPa)	Flow ($\frac{cm^3}{s}$)	Power (W)
white/red	34.47	37.80	1.305
red/black	34.47	51.66	1.784
black/grey	***34.47***	***57.33***	***1.979***
grey/brown	27.58	57.96	1.601
blue/white	48.26	36.54	1.766
blue/yellow	55.16	22.68	1.253

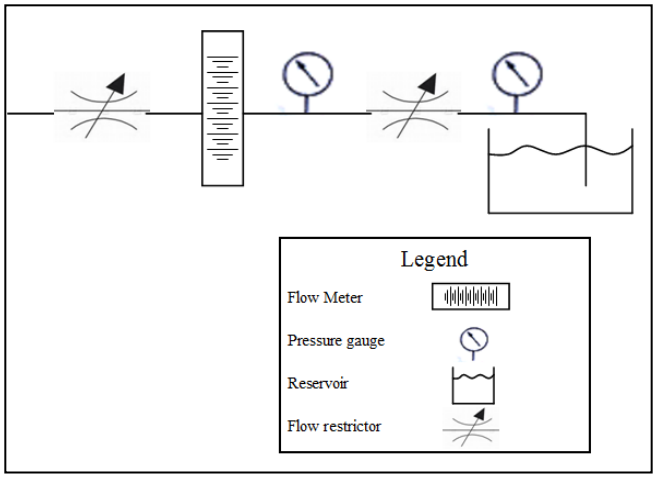

Fig. 6. Bench testing of flow versus pressure setup

4.2 System Optimization

Many of the components of the system have been optimized experimentally in order to produce the most power. Much of this optimization occurred during a series of dockside tests. Dockside testing utilized a cantilever arm and fulcrum, as shown in Fig. 7. The buoy was oscillated to match the design wave properties, a 3 second period and 0.5 meter height. The parameters tested were heave plate mass and configuration, hydraulic flow adjuster setting, and spring stiffness.

The mass of the heave plate was varied in 2.27 kg (5 lb) increments from 11.34 kg to 20.41 kg (25 to 40 lbs) and the output pressure peak and duration were compared via pressure gauge readings. Configurations of the heave plate that were tested included adding the cooking wok to the top side facing up, bottom side facing down, removed from the system, a 1.49 m^2 (16 ft^2) sheet of plywood added, and a 0.84 m^2 (9 ft^2) sheet of plywood added. The added drag from the plywood in both cases created slack in the line. The line stayed taut through the

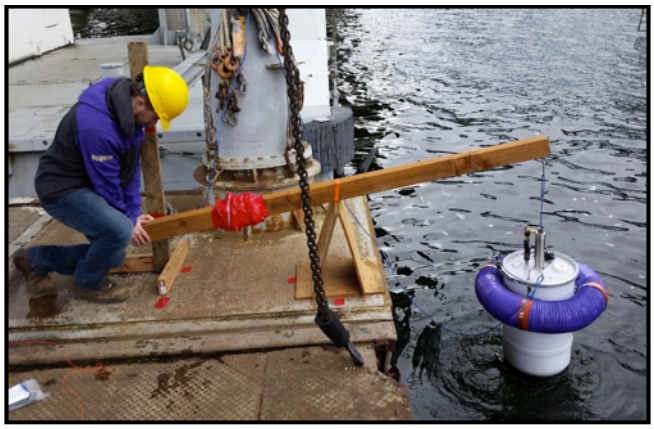

Fig. 7. Dockside testing of the WEC.

entire cycle with the wok in the upright position, leading

to the final heave plate design. The final total heave plate mass is 28.1 kg (62 lbs).

The needle valve controlling the hydraulic flow was optimized during dock testing. Each of the settings was tested, and the setting with the largest power output was chosen (the black/grey setting, highlighted in Table 1). Other parameters optimized in the hydraulic system were hydraulic fluid and tube size. Canola oil and water were tested in the system, but canola oil proved to provide much larger frictional losses, thus water was used in later tests. Tube sizes tested were 9.5 mm (3/8 inch) and 12.7 mm (1/2 inch). The 12.7 mm tube proved to lose less energy due to friction as compared to the 9.5 mm tube, thus the final system contains 12.7 mm tubing.

Maintaining line tension is critical in this design as slack can cause shock loading in the system. This can lead to failure of the line and loss of the heave plate. The stiffness of the spring plays a critical role in preventing shock loading, and the final spring rate used is 29.8 N/cm (17.0 lbs/in).

4.3 Buoy and Heave Plate Motion

The middle panel of Fig. 8 shows the displacement of the buoy and heave plate from static equilibrium during one set of waves. The WEC interacted with the wave from a time of 2 to 9 seconds. The buoy and heave plate oscillate with a period of approximately 2.1 seconds, and the heave plate lags the buoy by approximately 0.35 seconds. This corresponds to a phase lag of 60°. The IMU clocks drifted apart by about 3 seconds between when they were synchronized and the beginning of the test (3 days). Because of this, the buoy and heave plate IMU data sets were correlated under the reasonable assumption that the two IMUs began collecting data within 20 milliseconds of each other. The total change in distance between the two is approximately 23 cm, which is also the approximate range of motion of the hydraulic piston. A plot of this "slant" distance can be seen in the bottom panel of Fig. 8.

4.4 Hydraulic Power Output

Looking at the GoPro footage taken from the topside of the buoy, the pressure generated by the hydraulic system has been determined. The results of this can be seen in the top panel of Fig. 8. The maximum power output was 2.01 W, with an average power of 0.34 W, for the time that the buoy is interacting with the waves (~2-9 seconds).

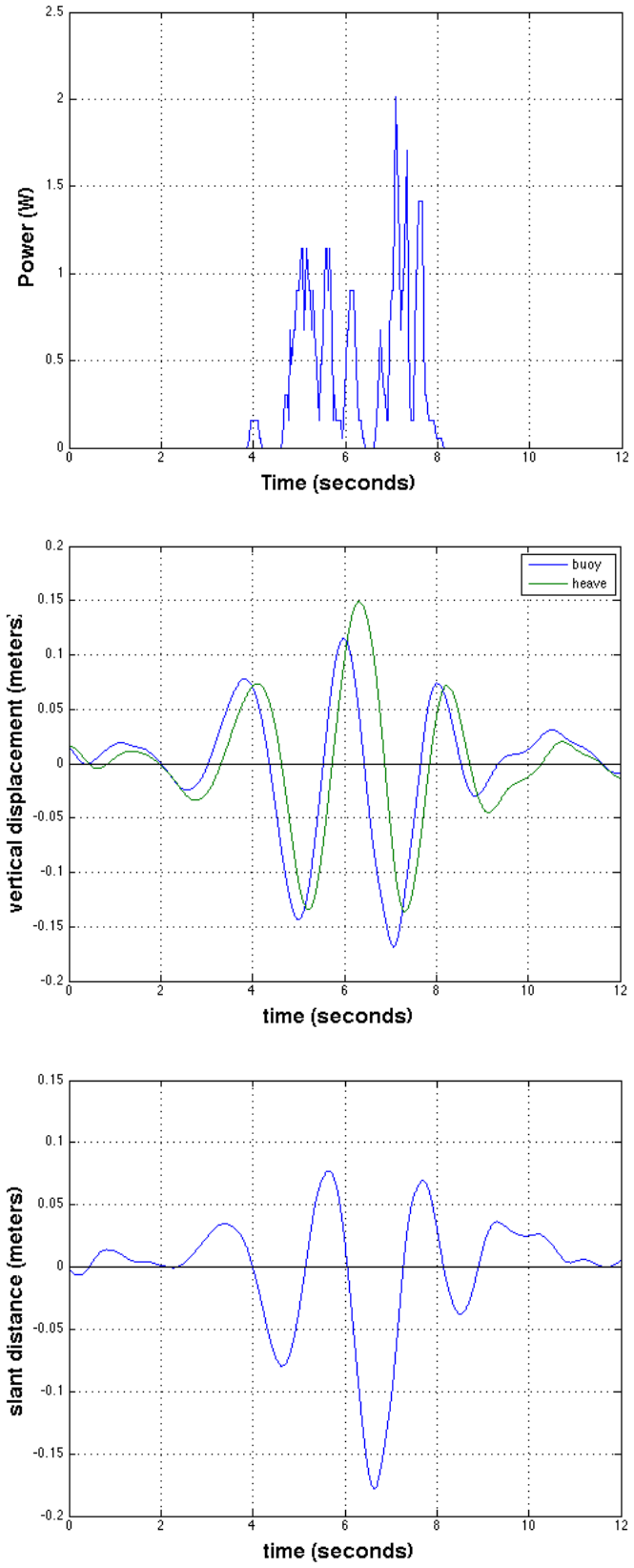

Fig. 8. Hydraulic power output (top), displacement of buoy and heave plate (middle), and slant displacement between buoy and heave plate (bottom) for lake test.

4.5 Incident Wave Power

Without accurate measurements from the SWIFTs, other methods were used to determine the parameters of the waves that the WEC interacted with. During the test, it was noted by the team that the buoy maintained a relatively constant waterline as it rode the waves, indicating that data from the motion of the buoy could be used to give a sense of the wave parameters.

Quantitatively, to determine whether the buoy tracked with the wave surface, the pressure logger data was examined. After calculating the depth as a function of time, the displacement of the buoy from its equilibrium position was determined by subtracting the mean depth from the data set. This yields the displacement of the bottom of the buoy from the wave surface. If the buoy displacement remained at zero for the entire test, it would indicate that the distance between the buoy pressure logger and the wave surface remained constant throughout the test. For the first three minutes of the lake test (Fig. A.4), it can be seen that this was not the case. There was displacement of the buoy from its mean depth and therefore a change in distance between the buoy bottom and wave surface. This was most likely due to the pitching of the buoy as the incident wave arrives, and also due to the imperfect movement of the buoy with the changing wave surface. It cannot be said that the buoy perfectly tracked with the waves for the entire duration of the test.

However, for the wave packet analyzed in this paper, it can be seen that the buoy displacement was small and the buoy followed the wave (Fig. A.5). In addition to the pressure logger data, footage from the GoPro cameras for this chosen wave section confirmed that the buoy closely followed the wave. For this wave packet, it can be concluded that the buoy tracked with the wave and that the relative displacement between the buoy and incident wave is close to zero. Thus, the height of the incident wave can be estimated from the displacement of the buoy, as determined by the IMUs.

Using this assumption, the incident wave power can be calculated. The boat wake may be approximated as a deep-water wave so long as the ratio of depth to wavelength is greater than 0.5. In this case, the depth is 60 meters, and the wavelength is close to 7 meters. Therefore, the ratio of depth to wavelength is 8.57, much greater than 0.5, so a deep-water approximation holds.

For a regular, deep-water wave, the wave power is calculated as

$$P_{regular,deep} = \frac{1}{32}\rho g^2 \frac{H^2 T}{\pi} \qquad (4)$$

where P is the wave power (W/m), ρ is the density of water (1000 kg/m^3), g is gravitational acceleration (9.81 m/s^2), H is the wave height (0.29 meters), and T is the wave period (2.1 seconds). Equation (4) gives a wave power of 169 W/m.

4.6 Heave Plate Dynamics

The drag force acting on the heave plate, as introduced in Section 3.5, is dependent on the direction that the heave plate is moving. The drag coefficient c_d can be approximated based on the shape of the heave plate. When the heave plate is moving in the negative Z direction, the flow is directed towards the convex side of the heave plate. For this situation, the type of object will be approximated as a hollow semi-sphere facing the stream, with $c_{d_{down}} = 0.38$. When the heave plate is moving in the positive Z direction, the flow is directed towards the concave side of the heave plate. For this situation, the heave plate can be approximated as a hollow semi-sphere opposite the stream, with $c_{d_{up}} = 1.42$.

The drag force can be determined by using Equation 3. The density of the fluid ρ is 1000 kg/m^3. The frontal area of the body, A, is equivalent to the cross sectional area of the heave plate. The cross sectional area of the semispherical heave plate is 0.936 m^2 (1451.47 in^2). The velocity is found using the IMU data. From this information, the drag force imparted by the heave plate on the system has been calculated. A plot of the drag force during the same wave packet analyzed previously can be seen in Fig. A.6.

4.7 Capture Width

For the wave train shown in Fig. 8, the estimated capture width, using Equation 2, is 0.002 m. As previously noted, there are large uncertainties in this calculation, but it is likely an accurate order-of-magnitude estimate.

5 Discussion

5.1 Position and Pressure Data

Correlating the pressure logger data with the IMU data, some of the finer dynamics of the system begin to appear. First, looking at the plot of hydraulic power from Fig. 8, it can be seen that, for the three waves in the wave set, the power output of the system increases for each consecutive wave. The design of the system is such that maximum power is achieved when the heave plate and buoy oscillate out of phase with one another. Before the wake hits, the buoy and heave plate "bob" more or less in-phase with each other. As the waves hit the device, the buoy and the heave plate begin to move out of phase with each other. It can be seen in the displacement plot of Fig. 8 that, as the buoy continues to be excited by more waves, the phase angle increases between the heave plate and buoy. This phase difference helps add to the power output of the system. This dynamic extends the displacement between the buoy and the heave plate, allowing for more extension of the hydraulic piston. Looking at the trend of the power plot (top panel in Fig. 8), it is noted that the peak power outputs seem to be increasing with each of the three waves. It is hypothesized that the peak power output for each wave in a regular wave field would level off at a value slightly higher than the peak power in the third wave. This would represent the system reaching its steady state. Since the current calculation of average power includes the build-up stages of the power plot, before the system has reached steady state, in a regular wave field, the system will most likely experience a higher average power. This will result in a larger capture width as well, since the capture width is dependent on the average power output of the system.

5.2 Scaling

Scaling to a full-scale WEC is non-linear, and can be estimated using Froude scaling. Per Holmes [5], power output for WECs scales to the power of 3.5 with geometric dimension. This means that, for a WEC five times larger, power output can be expected to be $5^{3.5}$ (~300) times larger than the original output, assuming that the wave conditions scale up similarly. For example, Froude scaling this WEC to a 5 meter diameter buoy suggests an average power of about 4 kW, and a peak power of 13 kW.

To get a sense of scale for the wave climates that these larger buoys would be expected to produce this power in, wavelengths would be scaled up linearly, and periods for the wave would be scaled to the power of 0.5 [5]. This means that, for the 5 meter buoy, wave heights would scale to 3.7 meters and periods to about 10.5 seconds, which are reasonable properties for ocean waves.

6 Future Work

Moving forward, there is much to still be analyzed about this system. Lake Washington provided little in terms of natural wave fields due to calm winds. Future goals for the current point absorber include testing the behavior in a natural wave field. This could help confirm data about system dynamics, providing a better understanding of the relative motion between the heave plate and buoy. Additionally, the system would be able to reach steady state in a natural wave field, thus a better idea of the power-producing capabilities of the device would be determined.

Future heave plate optimization will be targeted towards tuning the phase difference between buoy and heave plate motion to achieve the desired 90° phase angle. To achieve this, a flexible heave plate "skirt" will be tested, further increasing the directional-dependence of the heave plate drag. Additional dock testing may be pursued to test other heave plate designs before deploying them in Lake Washington.

Several improvements to instrumentation are needed. The instruments' clocks were not accurately synchronized at the time of deployment. Further, more accurate information about the relative motion of the buoy and heave plate could be determined with synchronized clocks. Additionally, a measurement of the tension in the line connecting the buoy to the heave plate would be useful. This would allow for much more accurate calculation of a number of heave plate parameters, and provide greater knowledge of the power entering the system. Accurate outside measurement of the wave climate would also prove useful when analyzing the system dynamics. If the system is tested in a natural wave field, SWIFT measurements should suffice.

7 Conclusion

A modular WEC was designed, optimized through dock testing, and field tested. The WEC experienced sets of

three boat wakes, with heights of 0.25 – 0.3 meters, and periods of about 2.1 seconds. The PTO produced 2.01 W at peak and 0.34 W on average. This results in an estimated capture width of about 2 mm. Moving forward, the buoy will undergo further testing, particularly testing in a natural wave field for a better understanding of its behavior.

8 References

[1] Jacobson, P. (2011). *Mapping and Assessment Of the United States Ocean Wave Energy Resource*. [ONLINE] Available at: http://www.boem.gov/Renewable-Energy-Program/Renewable-Energy-Guide/Ocean-Wave-Energy.aspx. [Accessed: 05-Jun-2015]

[2] Office of Energy Efficiency and Renewable Energy. 'Marine and Hydrokinetic Technology Glossary | Department of Energy', 2015. [Online]. Available: http://energy.gov/eere/water/marine-and-hydrokinetic-technology-glossary. [Accessed: 05-Jun- 2015].

[3] xioTechnologies. (2013, Oct 14). IMU-MATLAB-Library [Online]. Available: https://github.com/xioTechnologies/IMU-MATLAB-Library

[4] xioTechnologies. (2013, Nov 3). Oscillatory-Motion-Tracking-With-IMU [Online]. Available: https://github.com/xioTechnologies/Oscillatory-Motion-Tracking-With-IMU

[5] Holmes, Brian. "Tank Testing of Wave Energy Conversion Systems." The European Marine Energy Centre, Ltd. The British Library, 2009.

Appendix

Fig. A.1: Instrumentation attached to underside of buoy.

Fig. A.2: Heave plate instrumentation setup

Fig A.3: View of GoPro positioning on the buoy lid

Fig. A.4. Displacement of the buoy for the first three minutes of the lake test

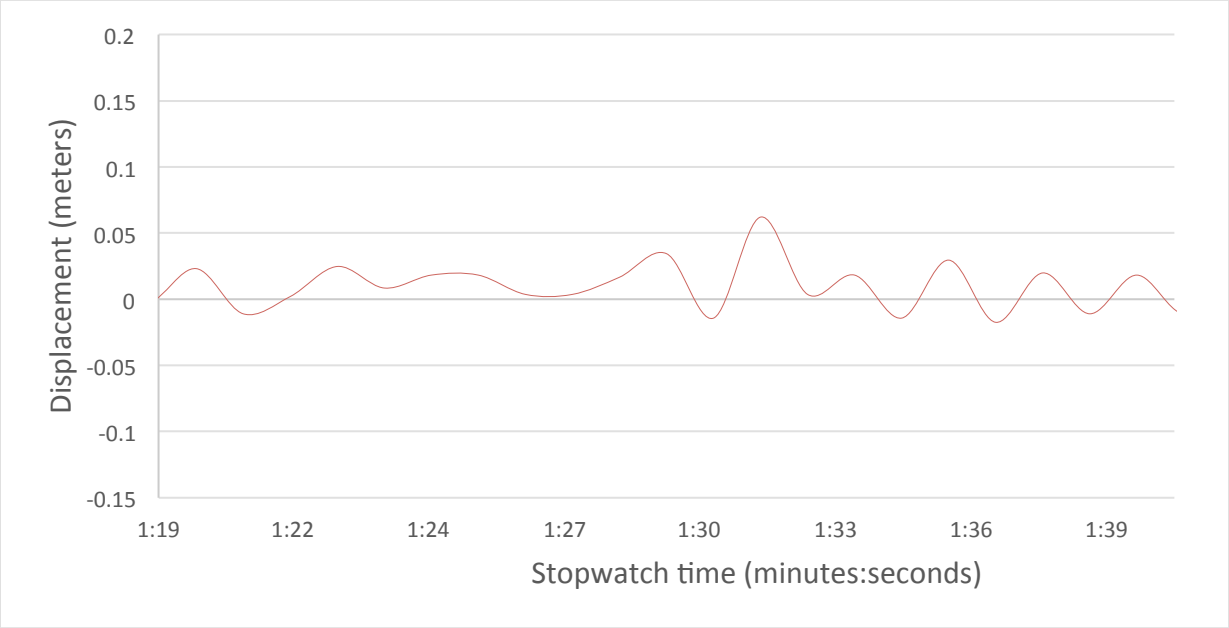

Fig. A.5. Displacement of the buoy from mean depth for one set of wakes

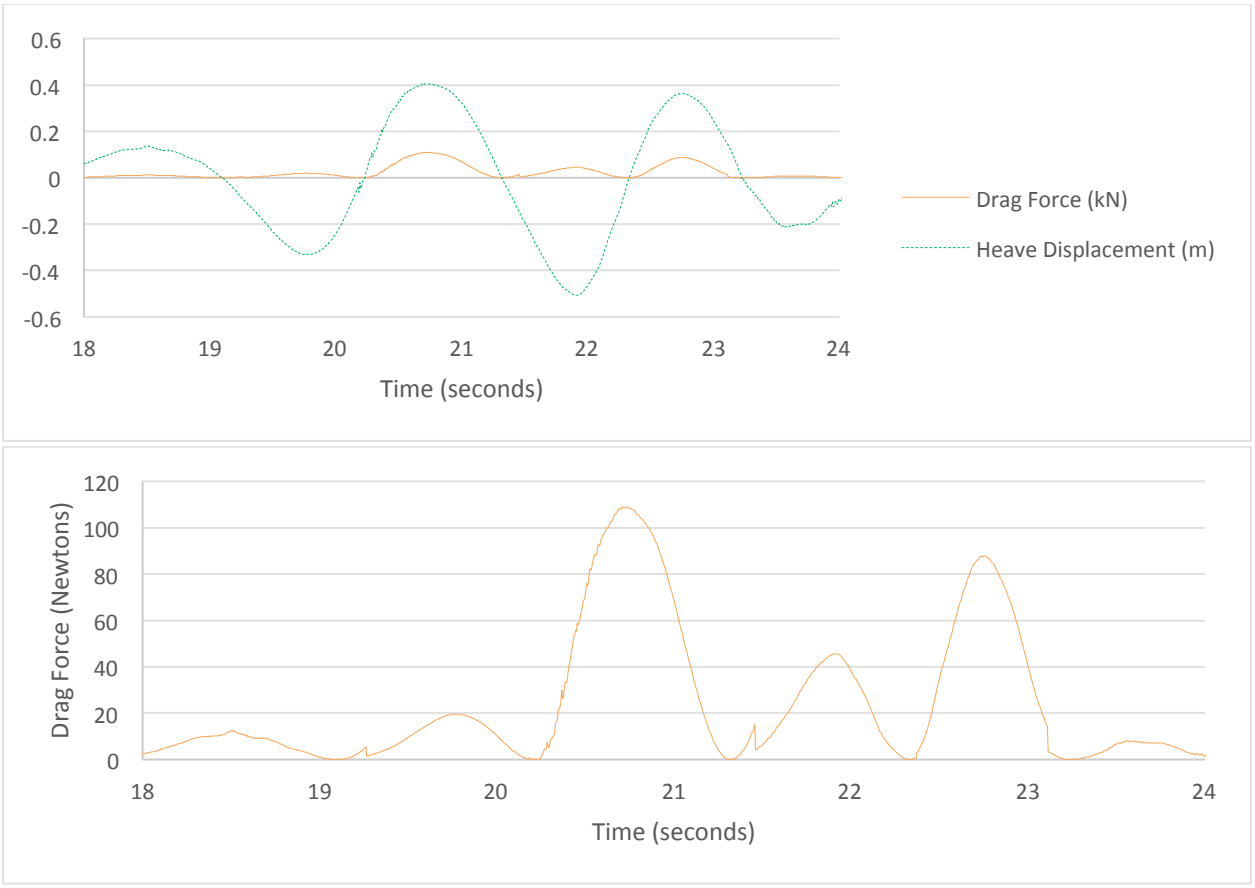

Fig. A.6. (Top) plot of the displacement of the heave plate overlapped with the drag force of the heave plate, and (bottom) a more detailed view of the drag force associated with the set of three wakes.